

Conf-910212--1

EFFECTS OF ATMOSPHERE AND HEATING RATE DURING
PROCESSING OF A CERAMIC SUPERCONDUCTOR*

FEB 21 1991

U. Balachandran, D. Xu, C. Zhang, S. E. Dorris, R. A. Russell, Y. Gao,+
K. L. Merkle,+ J. T. Dusek, J. J. Picciolo, and R. B. Poeppel
Materials and Components Technology Division
+Materials Science Division
Argonne National Laboratory
Argonne, IL 60439

and

CONF-910212--1

DE91 007761

G. Selvaduray
Department of Materials Engineering
San Jose State University
San Jose, CA 95192

January 1991

DISCLAIMER

This report was prepared as an account of work sponsored by an agency of the United States Government. Neither the United States Government nor any agency thereof, nor any of their employees, makes any warranty, express or implied, or assumes any legal liability or responsibility for the accuracy, completeness, or usefulness of any information, apparatus, product, or process disclosed, or represents that its use would not infringe privately owned rights. Reference herein to any specific commercial product, process, or service by trade name, trademark, manufacturer, or otherwise does not necessarily constitute or imply its endorsement, recommendation, or favoring by the United States Government or any agency thereof. The views and opinions of authors expressed herein do not necessarily state or reflect those of the United States Government or any agency thereof.

INVITED paper to be submitted for publication in the Proceedings of the Third International Symposium on High Temperature Superconductors: Processing and Microstructure Property Relationships, 1991 TMS Annual Meeting and Exhibition, New Orleans, LA, February 17-21, 1991.

*Work supported by the U. S. Department of Energy, Conservation and Renewable Energy, as part of a program to develop electric power technology, and Office of Basic Energy Sciences-Materials Science, under Contract W-31-109-Eng-38; and National Science Foundation, Office of Science and Technology Center, under Contract DMR88-09854.

DISTRIBUTION OF THIS DOCUMENT IS UNLIMITED

pc MASTER

EFFECTS OF ATMOSPHERE AND HEATING RATE DURING
PROCESSING OF A CERAMIC SUPERCONDUCTOR*

U. Balachandran, D. Xu, C. Zhang, S. E. Dorris, R. A. Russell, Y. Gao,+
K. L. Merkle,+ J. T. Dusek, J. J. Picciolo, and R. B. Poeppel
Materials and Components Technology Division

+Materials Science Department
Argonne National Laboratory
Argonne, IL 60439

and

G. Selvaduray
Department of Materials Engineering
San Jose State University
San Jose, CA 95192

Abstract

Properties of ceramic superconductors depend strongly on the temperature, heating rate, pressure, and atmosphere used during synthesis and fabrication. We have developed a process for synthesizing orthorhombic $\text{YBa}_2\text{Cu}_3\text{O}_x$ (123) superconducting powders by calcining the precursor powders under reduced total oxygen pressure. The resultant 123 powders are mixed with organics, and wires and coils are fabricated by extrusion. The wires and coils are fired at a reduced total pressure in flowing O_2 to reduce the concentrations of CO_2 , CO , and H_2O and thus prevent decomposition of the 123. Transport critical

current density of the superconductor decreases drastically with increasing concentrations of CO₂ in the gas mixture. Transmission electron microscopy of materials sintered in O₂ atmospheres containing various levels of CO₂ clearly shows the extent of grain boundary degradation.

Introduction

High-temperature ceramic superconductors are normally prepared via solid-state reaction from a mixture of precursors such as oxides, carbonates, and/or nitrates. The mixed precursors are calcined at 900-950°C for 50-100 h with intermittent grindings [1]. It is known that atmospheric contaminants such as CO₂ and H₂O can strongly affect the transition temperature, critical current density, and width of superconducting transition of YBa₂Cu₃O_x (123) superconductors [2-7]. Jahan et al. [8] indicated the formation of insulating phases when 123 reacts with water vapor, and several other researchers [1,5,6,8,9] have reported on the reaction of 123 with CO₂. During calcination of the precursor, simultaneous decomposition of BaCO₃ and reaction among the three constituent oxides form the desired superconducting phase. The CO₂ released by decomposition of BaCO₃ reacts with 123 and forms BaCO₃, Y₂O₃, CuO, and Y₂Cu₂O₅, depending on temperature [9]. The presence of these nonsuperconducting phases, especially at grain boundaries, lowers critical current density [11]. In addition, the conventional process is very time-consuming and results in coarse particles. We have developed a synthesis route to obtain essentially phase-pure orthorhombic 123 powders at 800°C in flowing O₂ at reduced pressure [12].

For many practical applications of high- T_c superconductors, it will be necessary to make long, continuous lengths of superconductor in a variety of shapes. Such lengths may possibly be fabricated by room-temperature plastic extrusion or fiber spinning [13-16], a powder-in-tube technique [17-20], or high-temperature extrusion process [21,22]. Since each method involves directional processing, development of favorable grain alignment is possible. The relationship of grain alignment to transport critical current density in high- T_c materials has been reviewed by Kroeger [23]. Plastic extrusion, in which the superconductor is mixed with organics and forced through a die under high pressure to form long lengths of wires and coils, leads to the evolution of relatively large amounts of CO_2 , CO , and H_2O during the removal of organic processing aids. It is therefore important to know the extent to which 123 decomposes in the presence of CO_2 and H_2O and whether such decomposition can be prevented by careful control of the furnace atmosphere.

In this paper, we describe a low pressure route to synthesize phase-pure 123. We also report on the degradation of properties (critical temperature, or T_c , and critical current density, or J_c) of 123 superconductors sintered in O_2 atmospheres containing CO_2 . The microstructures and compositions of the samples were investigated by transmission electron microscopy (TEM) and analytical electron microscopy (AEM). The relationships between the properties and the partial pressure of CO_2 are discussed in terms of the microstructural changes. In addition, we demonstrate that the sintering of 123 coils at reduced total pressure prevents its decomposition.

Experimental methods

Required amounts of Y_2O_3 , BaCO_3 , and CuO were wet-milled for about 15 h in methanol. The resultant slurry was pan-dried in air, ground in an agate mortar, and heated at a rate of $\approx 20^\circ\text{C}/\text{h}$ in the temperature range of $700\text{-}800^\circ\text{C}$ in flowing O_2 at a pressure of 2 mm Hg and held for 4 h at 800°C . During cooling, the vacuum was discontinued and ambient-pressure O_2 was passed. A 3-h hold at 450°C was incorporated into the cooling schedule to promote oxygenation of the resulting powder. A Fourier transform infrared (FTIR) spectrometer was used to monitor CO_2 evolution during calcination. Heating and O_2 flow rates were adjusted to maintain various levels of CO_2 during calcination. The calcined powders were characterized by thermal analyses and X-ray diffraction.

To examine the reaction between 123 and CO_2 in detail, pellets were pressed from the calcined powder and sintered in the temperature range of $900\text{-}1000^\circ\text{C}$ for about 5 h in flowing (≈ 1 atm) O_2/CO_2 gas mixtures. CO_2 concentration in the mixtures ranged from ≈ 0 to 5%. The samples were cooled slowly to room temperature, with a 12-h hold at 450°C to allow for reoxygenation. J_c was measured by a standard four-probe resistivity in liquid nitrogen. A criterion of $1 \mu\text{V}/\text{cm}$ was used for measurement of J_c . T_c values were obtained by resistivity and magnetization techniques. A low-field RF SQUID magnetometer was used for the magnetization measurements. Both TEM and AEM analyses were performed, with a Philips 420 Transmission analytical electron microscope operated at voltage of 120 kV. Thermogravimetric

analyses (TGA) were done on powders heated to $\approx 1000^\circ\text{C}$ in CO_2/O_2 gas mixtures.

Coils were fabricated from the calcined powder by plastic extrusion. In this technique, the ceramic powder was mixed with organic binder, solvent, dispersant, and plasticizer to form a homogenized plastic mass. This plastic mass was forced through a steel die having a narrow opening. The exiting wire from the die opening was wound over a mandrel to produce coils. Details of wire and coil fabrication have been given previously [24].

Results and discussion

TGA showed [Fig. 1, curve b] that during heating of the precursor powders at the ambient pressure of one atmosphere, the weight loss attributable to CO_2 evolution begins at about 750°C ; however, at 2 mm Hg, it begins at about 620°C . Under reduced total pressure, decomposition is essentially complete at $\approx 800^\circ\text{C}$, whereas under ambient pressure, decomposition is not complete even at $\approx 1000^\circ\text{C}$. Heating of powders at $\approx 20^\circ\text{C}/\text{h}$ in the range of $700\text{--}800^\circ\text{C}$ maintained CO_2 levels -- as measured by FTIR -- at less than 2% of the oxygen level. At 900°C under ambient pressure, the calculated thermodynamic equilibrium partial pressure of CO_2 at which La_2CuO_7 becomes unstable is $\approx 2\%$ in the oxygen atmosphere [9]. Faster heating rates resulted in higher CO_2 concentrations and yielded powders containing Y_2BaCuO_5 and other impurity phases. Endothermic or exothermic reactions or melting events associated with impurity phases were identified by differential thermal analysis (DTA) [1]. As shown in Fig. 2, for the powder calcined once at 800°C in low pressure, the only observed event was a change in slope caused by conversion of the powder from

orthorhombic to tetragonal upon heating (curve a). Conventionally processed powder (calcined three times at 900°C under ambient pressure) exhibited an endotherm at ≈940°C caused by melting of a CuO-BaCuO₂ eutectic (curve b). These traces were obtained in flowing oxygen at ambient pressure.

The 123 powder processed at low pressure was also shown to be phase-pure by X-ray diffraction. Analysis of the orthorhombic-peak split and comparison against published data [25] revealed no tetragonal phase in the powder. The particle size resulting from the low-pressure synthesis was 1 to 4 μm. This relatively small particle size is due to the low processing temperature. Calcination could be carried out at 800°C, rather than 900°C or higher, because cation diffusional kinetics in 123 are faster under reduced O₂ pressures [26]. Use of low oxygen partial pressure increases the concentration of oxygen vacancies in 123 [25,27,28]. A partial vacuum was used instead of a mixture of O₂ and a noble gas because CO₂ was removed with increased efficiency.

The resultant 123 powder was cold-pressed into pellets that were capable of levitating magnets. These pellets were then sintered in 1% O₂ (balance N₂) atmosphere at ≈900°C to make dense superconductors. Sintered pellet densities ranged from 88 to 94% of the theoretical value. Critical current densities, measured in zero applied magnetic field at 77 K were about 800 A/cm². The sintering temperature is lowered to ≈900°C compared to ≈950°C or higher because of the use of low partial pressure of O₂ (1% O₂). Low sintering temperature minimizes exaggerated grain growth and results in samples with small and uniform grain size.

In order to study the effect of CO₂ on the properties of 123, powder samples were heated on a TGA balance to ≈1000°C in 1% CO₂/99% O₂ gas mixture. The measured TGA data are shown in Fig. 3. There is an onset of weight gain at about 700°C, reaching a peak (≈4%) at ≈880°C, and a decline in weight at temperatures above ≈900°C. The onset temperature in TGA decreased with an increase in the fraction of CO₂ in the gas mixture. The increase in weight is due to formation of BaCO₃ (as a result of incorporation of CO₂) and other reaction products. At higher temperatures, BaCO₃ decomposes and accounts for the observed weight loss in Fig. 3.

The J_c values measured at 77 K in samples sintered in different CO₂/O₂ gas mixtures at various temperatures are given in Table 1. As the CO₂ partial pressure in the sintering atmosphere increased, J_c of sintered pellets decreased and finally became zero. Resistivity measurements showed that the materials with J_c = 0 were semiconducting. Magnetization measurements indicated that, even in the case of semiconducting samples, the major portion of the sample was still superconducting, and that the onset temperature of superconductivity was still ≈90 K. This can be seen in Fig. 4, where resistivity and magnetization data are given for two samples sintered at 940°C: one sample is a superconductor processed in 100% O₂ and the other is a semiconductor processed in 0.5% CO₂/O₂. The observed behavior could be explained if the superconducting current encountered a strong blockage in the semiconducting sample. A possible cause of the blockage could be a thin layer of non-superconducting secondary phases at grain boundaries, formed by the reaction of 123 with CO₂ in the gas mixtures during sintering. Because the grain interiors are not degraded, a sharp change in magnetization is

seen at ≈ 90 K in the samples that showed semiconducting behavior in the resistivity measurements (Fig. 4).

These arguments are supported by TEM observations [6,7], which show the presence of secondary phases at some grain boundaries. An example of one such grain boundary is shown in Fig. 5 for the sample sintered at 970°C in 0.5% CO_2/O_2 gas mixture. X-ray energy-dispersive spectroscopy (XEDS) shows that the grain-boundary material consists of BaCuO_2 and $\text{Y}_2\text{Cu}_2\text{O}_5$. The width of this grain-boundary material is much greater than the coherence length in 123, thus it can completely obstruct the superconducting current and cause a reduction in overall critical current density. However, this type of grain boundary accounts for only about 10% of the observed grain boundaries; the majority appear quite sharp with no obvious evidence of a second phase. Because of the multitude of possible percolation paths, the value of J_c would not become zero if only 10% of the grain boundaries were coated with a second phase. For the superconducting current to be completely blocked, as in the case of the semiconducting samples, a majority of the grain boundaries must be nonsuperconducting. High-resolution electron microscopy (HREM) images of the grain boundaries suggested that, in fact, the majority of grain boundaries probably are nonsuperconducting.

Careful study of the HREM images showed that the structure near the sharp grain boundaries is not orthorhombic but some other phase, possibly tetragonal 123. Figure 6 shows a HREM image in which lattice fringes of (001) planes are clearly observed in one grain. Through careful measurement of the interplanar spacing, it was found that the spacing is about 1.19 nm in the regions near grain boundaries, whereas

the spacing is approximately 1.17 nm in the regions far from the grain boundaries. Neutron diffraction data [29] show that tetragonal 123 has $c = 1.19$ nm. Another indication of tetragonal material is the termination of twinning near the grain boundaries, which can be taken as the demarcation line between orthorhombic and tetragonal structures because the tetragonal structure has no twins.

A possible explanation for the phase transformation from orthorhombic to tetragonal is the incorporation of carbon into the lattice due to the presence of CO_2 in the sintering atmosphere [6,7]. Segregation of carbon at grain boundaries or in regions near grain boundaries has been confirmed in a previous study [6] using secondary ion mass spectroscopy (SIMS). Carbon can diffuse into the lattice and expel oxygen from the orthorhombic structure, thus forming a nonsuperconducting tetragonal structure that can block the superconducting current. We observed that in most cases, such tetragonal regions near grain boundaries vary in size from a few nanometers to several tens of nanometers. Therefore, they are very difficult to detect and are not readily identifiable in most boundaries.

In view of this, the effect of residual carbon on the processing and properties of extruded coils must be considered. In the green state, superconducting coils contain ≈ 10 wt.% organics that must be completely removed without damaging the superconductor. Incomplete removal of the organics can cause decomposition of the superconductor or leave carbon-rich material at the grain boundaries, either of which will degrade superconducting properties. Organics can be easily removed by thermal decomposition in the temperature range of 240–350°C, but if the decomposition proceeds too rapidly, the coils can bloat

severely and in some cases even explode. Also, decomposition of organics produces significant concentrations of H₂O and CO₂, which, as we have seen, can react with 123; therefore, the rate of organic removal must be carefully controlled.

When superconducting coils are sintered at a reduced total pressure in flowing O₂, the CO₂ and H₂O are removed as they are produced, thereby minimizing their concentrations in the atmosphere surrounding the coils and preventing decomposition of 123. But when coils are sintered at ambient pressure O₂, the harmful gaseous products accumulate and lead to the decomposition of 123. To demonstrate this, mixtures made from 123 powder and the same organics used in extrusion were heated in flowing oxygen at either ambient or reduced pressure (≈ 2 mm Hg). Two different powders were used: powder produced by solid-state reaction at reduced pressure and powder produced by a liquid-mix technique. Samples were taken from the mixtures at 240, 300, and 350°C, and their X-ray patterns were obtained. Figures 7 and 8 are schematic illustrations of the major peaks in these patterns. Figure 7 shows that, when the 123/organic mixtures were heated at ambient pressure, both samples of 123 decomposed (the liquid-mix powder at 240°C and the solid-state powder at 300°C). Figure 8 shows, however, that gross decomposition of 123 did not occur when the mixtures were heated at reduced total pressure, even though the relative intensities of peaks varied as a result of changing oxygen content.

Shown in Table 2 are the sintering conditions and properties of five coils made by extrusion and heated at reduced total pressure in flowing O₂. During binder removal, these coils are heated at a rate of $\approx 5^\circ\text{C}/\text{h}$ in

the temperature range 150-400°C. Figure 9 shows the photograph of a five layer, seventy five turn, 123 coil coated with Y_2BaCuO_5 (211, so-called "green phase") insulator. This coil was heated in flowing O_2 at a total pressure of 10 mm Hg. Although the critical current densities are well below those necessary for many large-scale applications, it should be noted that the length of continuous superconductor in these coils ranges up to ≈ 12 m. Moreover, the measurements were made in magnetic fields of up to 73 G, and fringing effects at the coil ends probably increase the field on the end turns even further. Considering that just a few years ago it was not possible to obtain such performance consistently on even short lengths of superconductor in zero field, these results represent significant improvement in bulk superconductor fabrication. Although large differences in size and geometry make it difficult to compare the J_c results of pellets and coils, a comparison of J_c in Tables 1 and 2 suggests that CO_2 evolved during removal of organics from the coils had minimal impact on superconducting properties when sintering was at reduced total pressure. Keeping in mind that the J_c of bulk materials drops dramatically with magnetic field and that the coils were measured in fields up to at least 73 G, we suggest that the coil results agree most closely with the results for pellets sintered in 100% O_2 . This indicates further that large multilayer superconducting coils can be successfully fabricated by sintering at reduced total pressure, and that these coils have superconducting properties that are representative of bulk materials.

Conclusions

Solid-state reaction remains the simplest technique for synthesizing 123 superconductors. Use of BaCO_3 , which is not hygroscopic, obviates the need for processing in carefully controlled humidity. A single calcination at 800°C for 4 h in reduced total oxygen pressure gives essentially phase-pure, orthorhombic 123 powders. The reaction temperature is about $100\text{-}150^\circ\text{C}$ lower than that used in ambient-pressure calcination, and the lower temperature results in finer particles. 123 reacts strongly with CO_2 at high temperatures, leaving superconducting grain interiors encased in nonsuperconducting grain boundary phases. These secondary phases obstruct superconducting currents and cause a decrease in J_c . Carbon becomes segregated at the grain boundaries and causes the material near the grain boundaries to transform from the orthorhombic phase to the nonsuperconducting tetragonal phase. In the sintering of large multilayer coils, CO_2 concentration can be minimized and 123 decomposition can be avoided by heating at reduced total pressure. As a result, superconducting coils can be fabricated that produce magnetic fields up to 73 G with an air core and 330 G with an iron core.

Acknowledgments

*This work was supported by the U.S. Department of Energy, Conservation and Renewable Energy, as part of a program to develop electric power technology, and the Office of Basic Energy Sciences - Materials Science, under Contract W-31-109-Eng-38; and by the National Science Foundation, Office of Science and Technology Center, under Contract DMR88-09854.

References

1. K. C. Goretta, I. Bloom, N. Chen, G. T. Goudey, M. C. Hash, G. Klassen, M. T. Lanagan, R. B. Poeppel, J. P. Singh, D. Shi, U. Balachandran, J. T. Dusek, and D. W. Capone II, "Calcination of $\text{YBa}_2\text{Cu}_3\text{O}_{7-x}$ powder," *Mater. Lett.*, **7**, 161 (1988).
2. P. K. Gallagher, G. S. Grader, and H. M. O'Bryan, "Some effects of CO_2 , CO , and H_2O upon the properties of $\text{YBa}_2\text{Cu}_3\text{O}_7$," *Mat. Res. Bull.*, **23** (10), 1491-1499 (1988).
3. E. K. Chang, E. F. Ezell, and M. J. Kirschner, "The effect of CO_2 in the processing atmosphere of $\text{YBa}_2\text{Cu}_3\text{O}_x$," *Supercond. Sci. Technol.*, **8**, 391-394 (1990).
4. T. B. Lindemer, C. R. Hubbard, and J. Brynstad, " CO_2 solubility in $\text{YBa}_2\text{Cu}_3\text{O}_{7-x}$," *Physica C.*, **167**, 312-316 (1990).
5. T. M. Shaw, D. Dimos, P. E. Batson, A. G. Schrott, D. R. Clarke, and P. R. Duncombe, "Carbon retention in $\text{YBa}_2\text{Cu}_3\text{O}_{7-x}$ and its effect on the superconducting transition," *J. Mater. Res.*, **5** (6), 1176-1184 (1990).
6. Y. Gao, K. L. Merkle, C. Zhang, U. Balachandran, and R. B. Poeppel, "Decomposition of $\text{YBa}_2\text{Cu}_3\text{O}_{7-x}$ during annealing in CO_2/O_2 mixtures," *J. Mater. Res.*, **5** (7), 1363-1367 (1990).

7. Y. Gao, Y. Li, K. L. Merkle, J. N. Mundy, C. Zhang, U. Balachandran, and R. B. Poeppel, "J_c degradation of YBa₂Cu₃O_{7-x} superconductors sintered in CO₂/O₂," Mater. Lett., **9** (10), 347-352 (1990).
8. M. S. Jahan, D. W. Cooke, H. Sheinberg, J. L. Smith, and D. P. Lianos, "Environmental effects on luminescence yield of superconducting YBa₂Cu₃O_x," J. Mater. Res., **4** (4), 759-762 (1989).
9. H. Fjellvag, P. Karen, A. Kjekshus, P. Kofstad, and T. Norby, "Carbonatization of YBa₂Cu₃O_{6+x}," Acta Chem. Scand., **A42**, 178-184 (1988).
10. E. A. Cooper, A. K. Gangopadhyay, T. O. Mason, and U. Balachandran, "CO₂ decomposition kinetics of YBa₂Cu₃O_{7-x} via in situ electrical conductivity measurements," submitted to J. Mater. Res., September, 1990.
11. D. Shi, D. W. Capone II, G. T. Goudy, J. P. Singh, N. J. Zaluzec, and K. C. Goretta, "Sintering of YBa₂Cu₃O_{7-x} compacts," Mater. Lett., **6**, 217 (1988).
12. U. Balachandran, R. B. Poeppel, J. E. Emerson, S. A. Johnson, M. T. Lanagan, C. C. Youngdahl, Donglu Shi, K. C. Goretta, and N. G. Eror, "Synthesis of phase-pure orthorhombic YBa₂Cu₃O_x under low oxygen pressure," Mater. Lett., **8** (11,12), 454-456 (1989).

13. S. Lee, B. Taylor, and J. Vrba, "The fabrication of a ceramic superconducting wire," *Supercon. Sci. Technol.*, **1**, 137-140 (1988).
14. Y. Tanaka, K. Yamada, and T. Sano, "YBCO superconducting coils operated at nitrogen temperature," *Jpn. J. Appl. Phys.*, **27** (5), L799-L801 (1988).
15. R. B. Poeppel, S. E. Dorris, C. A. Youngdahl, J. P. Singh, M. T. Lanagan, U. Balachandran, J. T. Dusek, and K. C. Goretta, "Shape forming high- T_c superconductors," *J. Met.*, **41** (1), 11-13 (1989).
16. K. C. Goretta, M. T. Lanagan, J. P. Singh, J. T. Dusek, U. Balachandran, S. E. Dorris, and R. B. Poeppel, "Fabrication of high- T_c superconductors," *Mater. Manufact. Proc.*, **4**, 163-175 (1989).
17. H. Sekine, K. Inoue, H. Maeda, K. Numata, K. Mori, and H. Yamamoto, "Fabrication of multifilamentary YBCO superconductors," *Appl. Phys. Lett.*, **52** (26), 2261-2262 (1988).
18. K. Heine, J. Tenbrink, and M. Thoner, "High field critical current densities in $\text{Bi}_2\text{Sr}_2\text{Ca}_1\text{Cu}_2\text{O}_{8+x}/\text{Ag}$ wires," *Appl. Phys. Lett.*, **55** (23), 2441-2443 (1989).
19. D. Shi and K. C. Goretta, "Swaged superconducting wires," *Mater. Lett.*, **7** (12), 428-432 (1989).

20. S. X. dou, H. K. Liu, M. H. Apperly, K. H. Song, and C. C. Sorrell, "Critical current density in superconducting Bi-Pb-Sr-Ca-Cu-O wires and coils," *Supercond. Sci. Technol.* **3**, 138-142 (1990).
21. S. K. Samanta, "Manufacturing of high- T_c superconducting ceramic wire by hot extrusion," paper presented at the TMS Annual Meeting, Las Vegas, NV, 27 February, 1989.
22. K. Rajan, W. Misiolek, R. Garcia, and R. N. Wright, "Hot extrusion of $YBa_2Cu_3O_{7-x}$," pp. 291-299, in "High temperature superconducting compounds II," ed. by S. H. Whang, A. DasGupta, and R. Laibowitz, TMS Publications, Warrendale, PA, 1990.
23. D. M. Kroeger, "Grain boundaries and J_c in high- T_c oxide superconductors," *J. Met.*, **41** (1) 14-17 (1989).
24. S. E. Dorris, J. T. Dusek, J. J. Picciolo, R. Russell, J. P. Singh, and R. B. Poeppel, " $YBa_2Cu_3O_x$ superconductor coil: Processing and properties," *Proceedings of the International Conference on Electrical Machines (ICEM)*, Cambridge, MA, August, 1990, in press.
25. W. Wong-Ng, R. S. Roth, L. J. Swartzendruber, L. H. Bennett, C. K. H. Chiang, F. Beech, C. R. Hubbard, "X-ray powder characterization of $Ba_2YCu_3O_{7-x}$," *Adv. Ceram. Mater.*, **2** (3B), 565-576 (1987).

26. A. W. von Stumberg, N. Chen, K. C. Goretta, and J. L. Routbort, "High-temperature deformation of $\text{YBa}_2\text{Cu}_3\text{O}_{7-x}$," *J. Appl. Phys.*, **66**, 2079-2082 (1989).
27. P. K. Gallagher, "Characterization of $\text{Ba}_2\text{YCu}_3\text{O}_x$ as a function of oxygen partial pressure Part I: Thermodynamical measurements," *Adv. Ceram. Mater.*, **2** (3B), 632-639 (1987).
28. F. Beech, A. Miraglia, A. Santoro, and R. S. Roth, "Neutron study of the crystal structure and vacancy distribution of the superconductor $\text{Ba}_2\text{YCu}_3\text{O}_{9-x}$," *Phys. Rev. B.*, **35**, 8778-8786 (1987).
29. J. D. Jorgensen, M. A. Beno, D. G. Hinks, L. Soderholm, K. J. Volin, R. L. Hitterman, J. D. Grace, I. K. Schuller, C. U. Segre, K. Zhang, and M. S. Kleefisch, "Oxygen ordering and the orthorhombic-to-tetragonal phase transition in $\text{YBa}_2\text{Cu}_3\text{O}_{7-x}$," *Phys. Rev.* **B36**, 3608-3616 (1987).

Table Captions

Table 1. Relative densities and transport J_c (77 K) for samples sintered over a range of temperatures in various CO_2/O_2 mixtures.

Table 2. Sintering conditions and properties of superconducting coils.

Figure Captions

Figure 1. Change in mass observed by thermogravimetric analysis during heating of 123 precursor powders: (a) 2 mm Hg pressure; (b) ambient pressure.

Figure 2. Differential thermal analysis traces of 123 powder (a) calcined at 2 mm Hg pressure and (b) at ambient pressure.

Figure 3. Thermogravimetric trace of 123 heated to $\approx 1000^\circ\text{C}$ in 1% $\text{CO}_2/99\% \text{O}_2$ gas mixture.

Figure 4. Resistivity versus temperature (a), and magnetization versus temperature (b) for two samples fired at 940°C (Sample 1 was fired in 100% O_2 ; Sample 2 was fired in 0.5% CO_2/O_2).

Figure 5. TEM micrograph of grain boundary (GB) in 123 sample sintered at 970°C in 0.5% CO_2/O_2 atmosphere. Thick second-phase layer is identified as BaCuO_2 .

Figure 6. High resolution electron micrograph of a grain boundary in a 123 sample sintered at 970°C in 0.5% CO₂/O₂ gas mixture. The region near the grain boundary has a tetragonal structure while the region away from the grain boundary has an orthorhombic structure. Note that the twin structure is terminated at the tetragonal region.

Figure 7. Schematic X-ray patterns of fully oxygenated 123 powder (as reference) and two other 123 powders heated to the indicated temperature at *ambient pressure* in contact with the organics used in extrusion of coils. The patterns show that both powders fired with the organics decomposed during heating.

Figure 8. Schematic X-ray patterns of 123 powder as a function of temperature. The powder was heated to the indicated temperature at *reduced total pressure* in contact with the organics used in extrusion of coils. The patterns reveal no indication of decomposition.

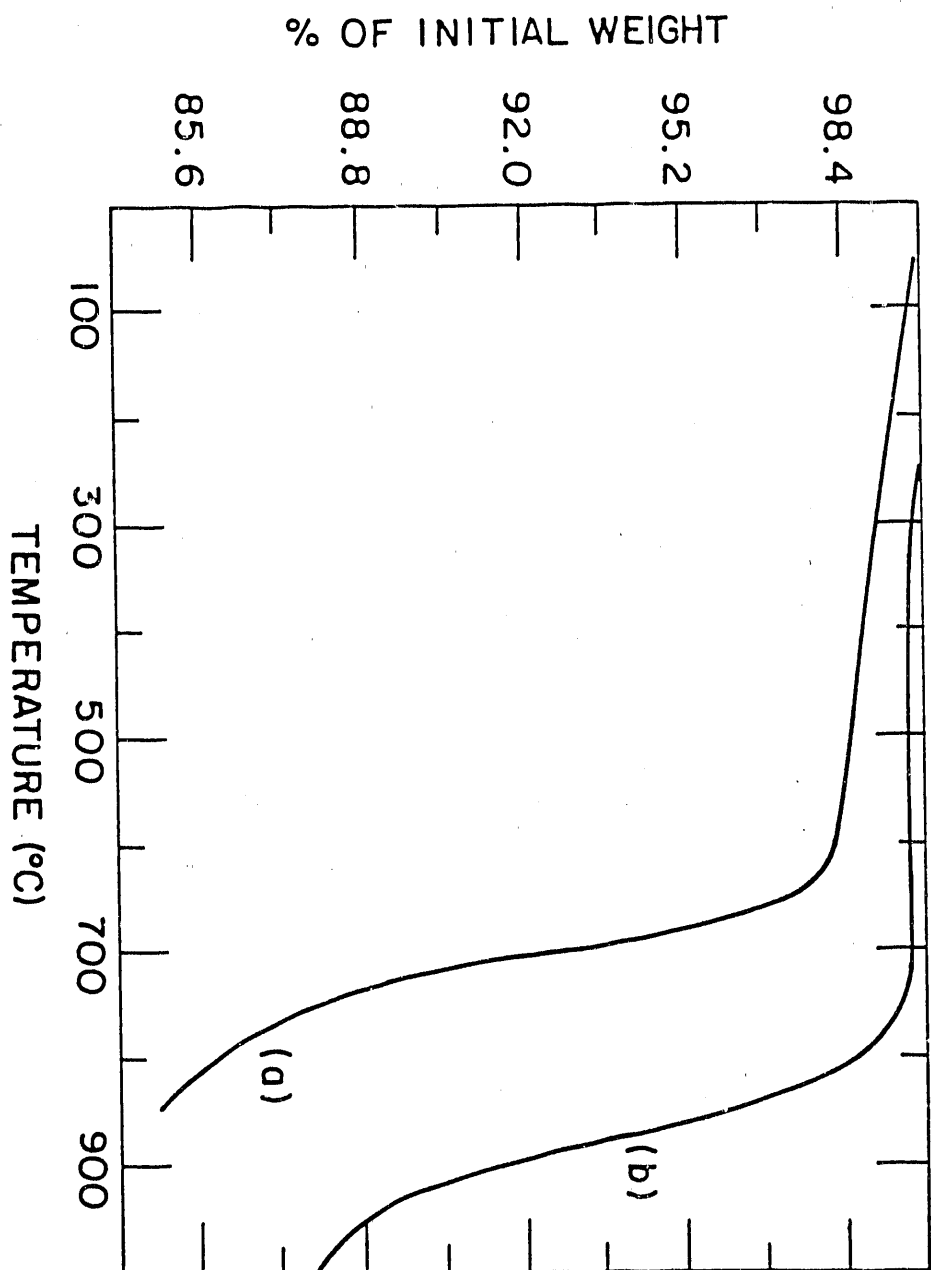
Figure 9. Photograph of a five layer, seventy five turn 123 coil coated with insulating 211 green phase. Total length of wire in this coil is about 12 m and it has been sintered in flowing O₂ at a pressure of 10 mm Hg.

Table 1. Relative densities and transport J_c (77 K) for samples sintered over a range of temperatures in various CO_2/O_2 mixtures.

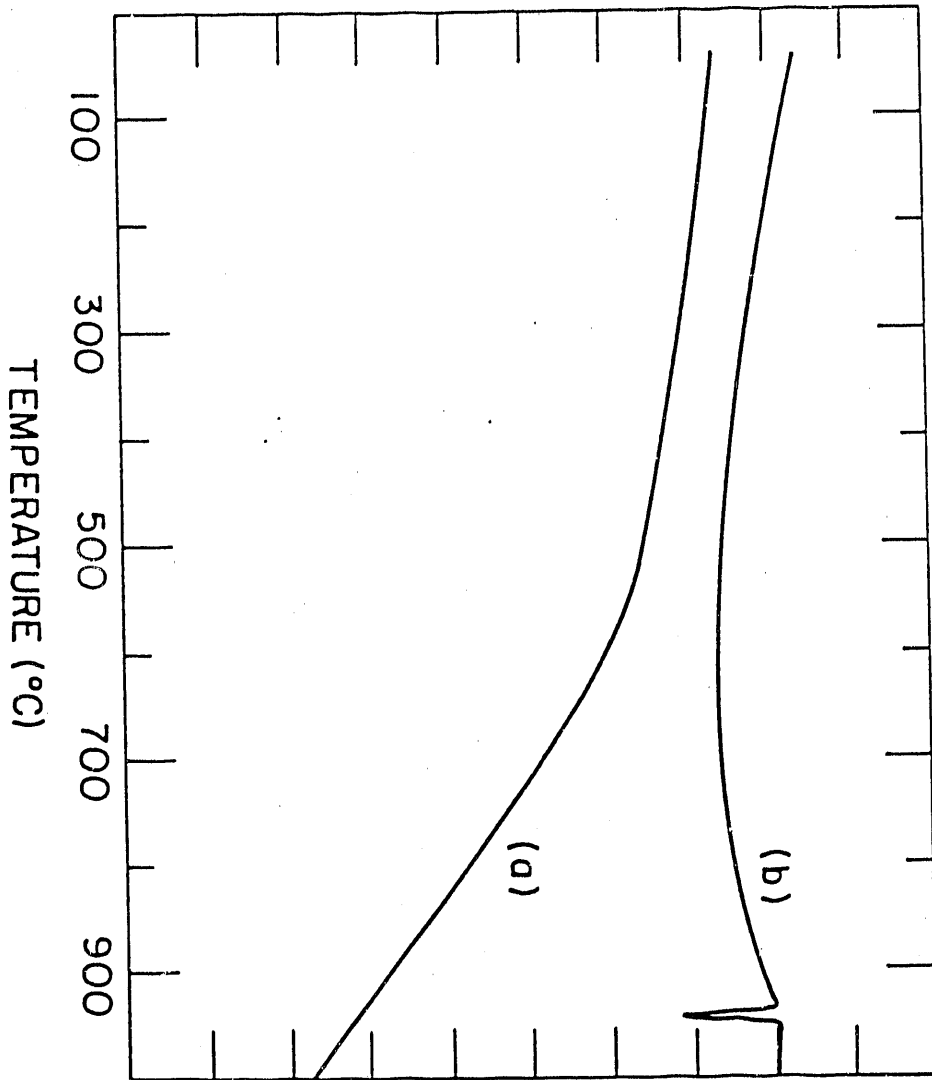
Sintering Temp.	CO_2 (%)	Density (%)	J_c (A/cm ²)
1000 °C	0	93	320
	0.005	92	157
	0.05	92	106
	0.5	92	34
	5.0	93	0
970 °C	0	87	315
	0.005	86	138
	0.05	90	94
	0.5	86	0
	5.0	87	0
940 °C	0	67	128
	0.005	67	21
	0.05	68	0
	0.5	66	0
	5.0	-	-
910 °C	0	63	60
	0.005	62	0
	0.05	63	0
	0.5	62	0
	5.0	-	-

Table 2. Sintering conditions and properties of superconducting coils.

<u>Coil Description</u>	<u>Firing Conditions</u>	<u>J_c (A/cm²)</u>	<u>B (Gauss)</u>	<u>B(Fe Core) (Gauss)</u>
<u>Coil #1</u> Uncoated 25 Turns	100% O ₂ 910°C	120	19	---
<u>Coil #2</u> 211-Coated 25 Turns	100% O ₂ 910°C	130	20	---
<u>Coil #3</u> Uncoated 21 Turns	2 mm Hg 875°C	225	36	---
<u>Coil #4</u> 211-Coated 2 Layers 42 Turns	10 mm Hg 875°C	150	42	160@77K
<u>Coil #5</u> 211-Coated 5 Layers 75 Turns	10 mm Hg 875°C	150	73	330@77K 420@73K



ΔH (arb. units)



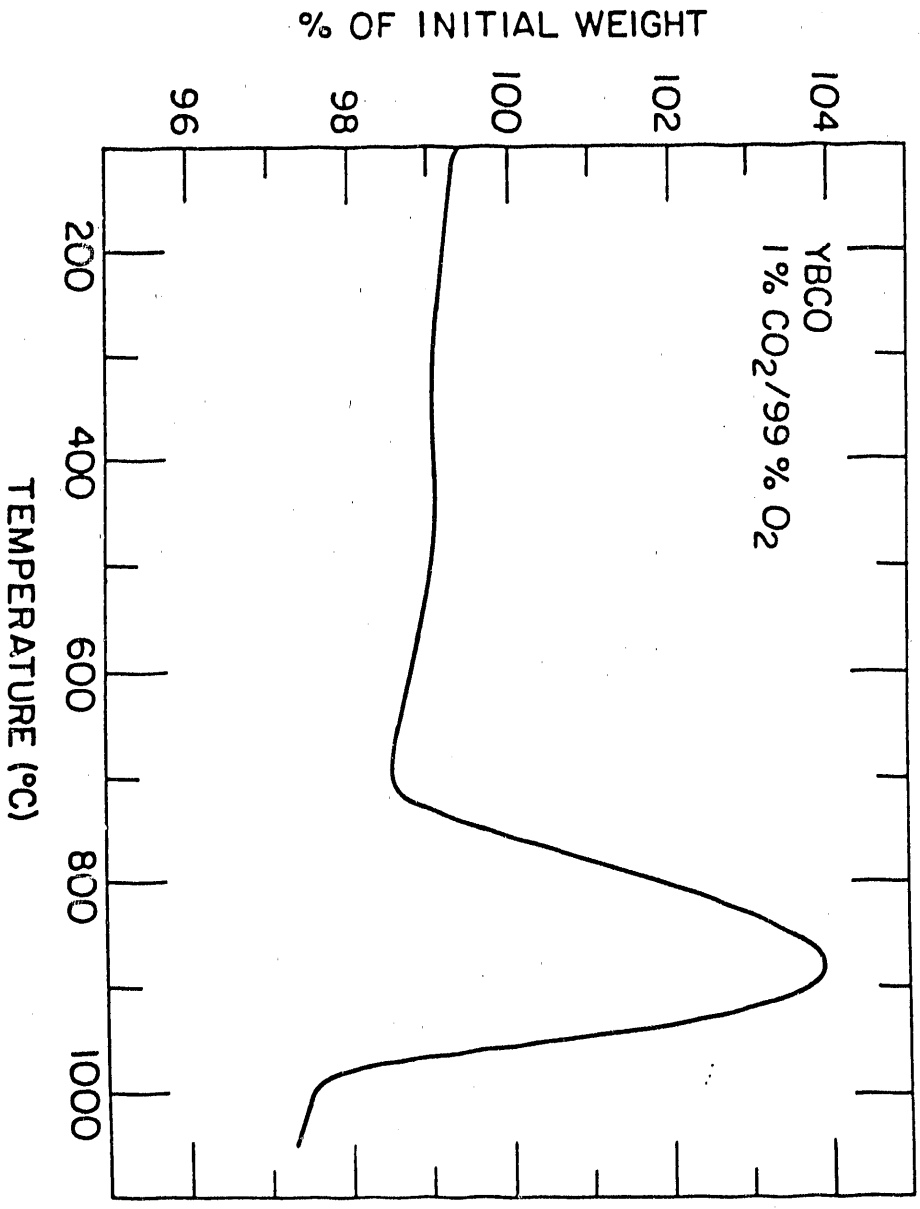


Figure 3

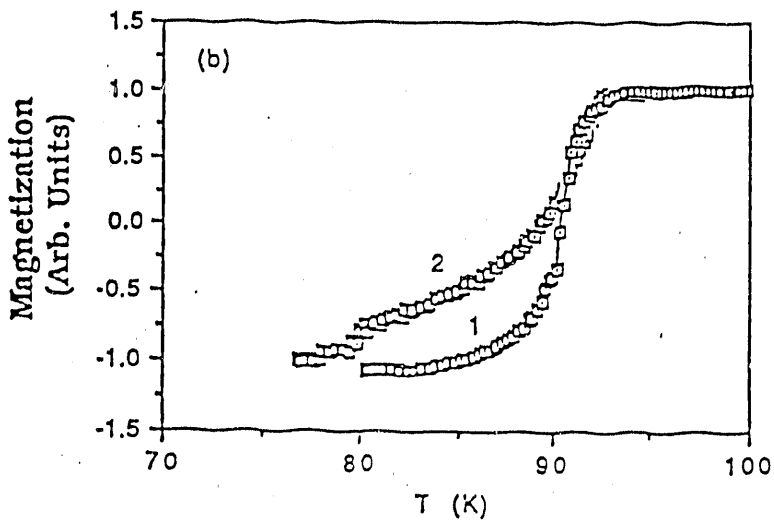
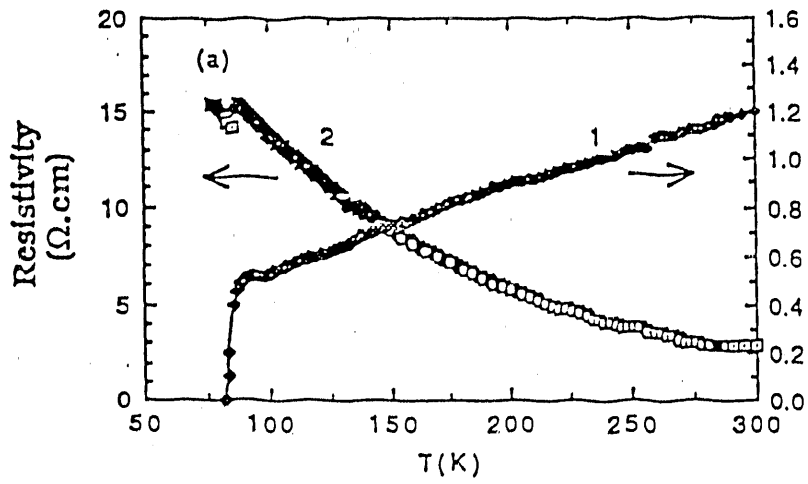


Figure 4

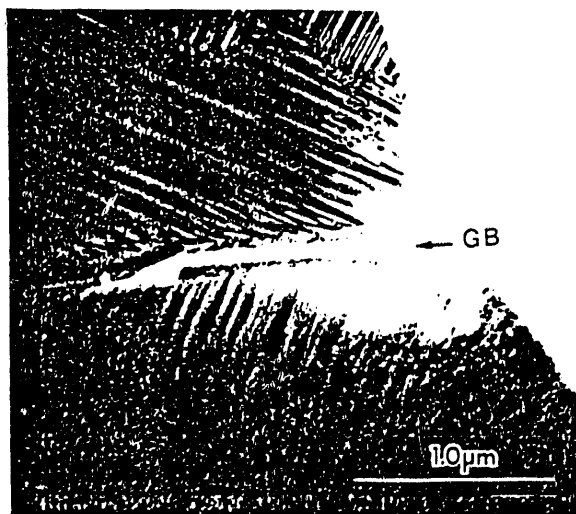
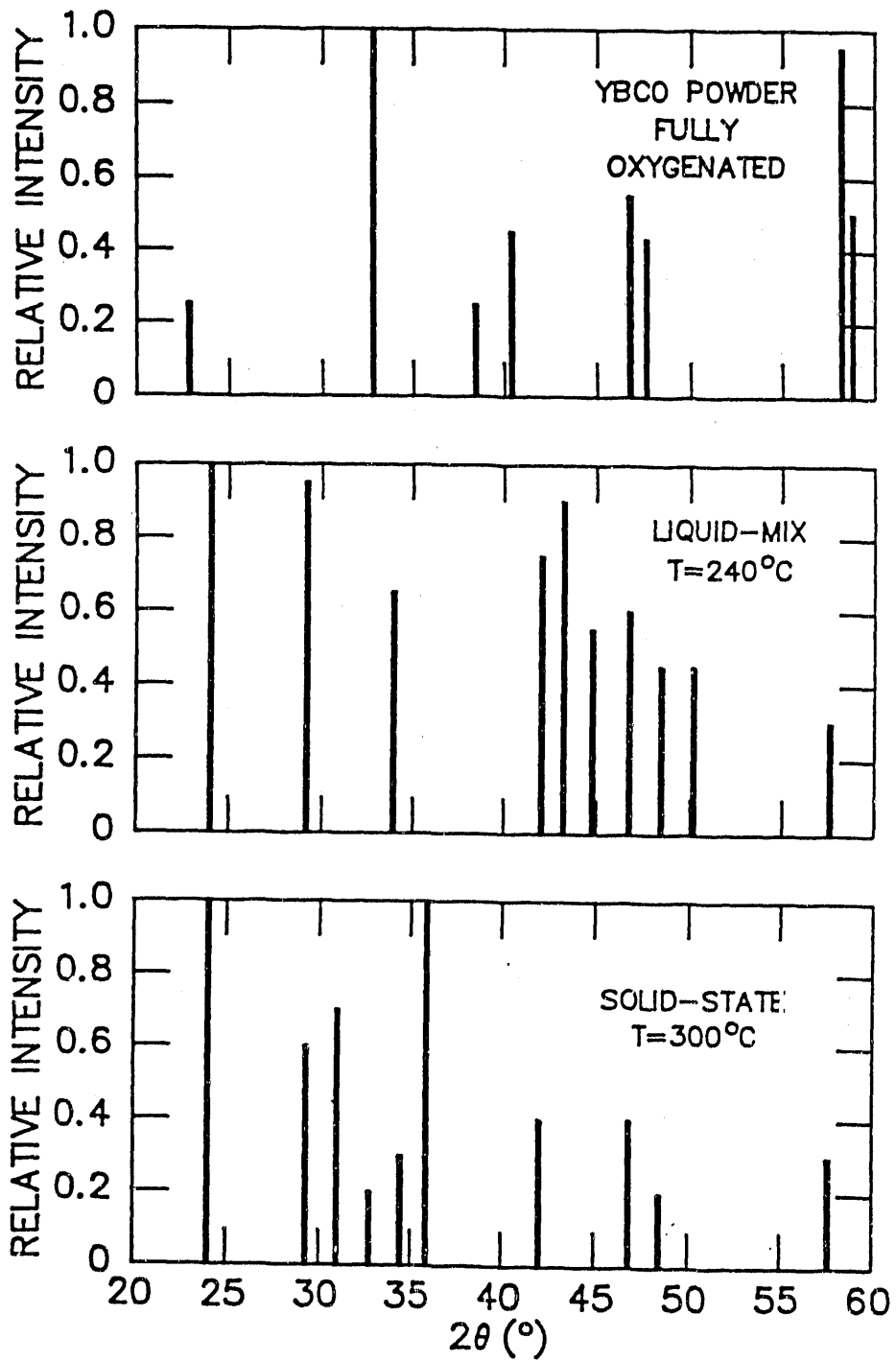


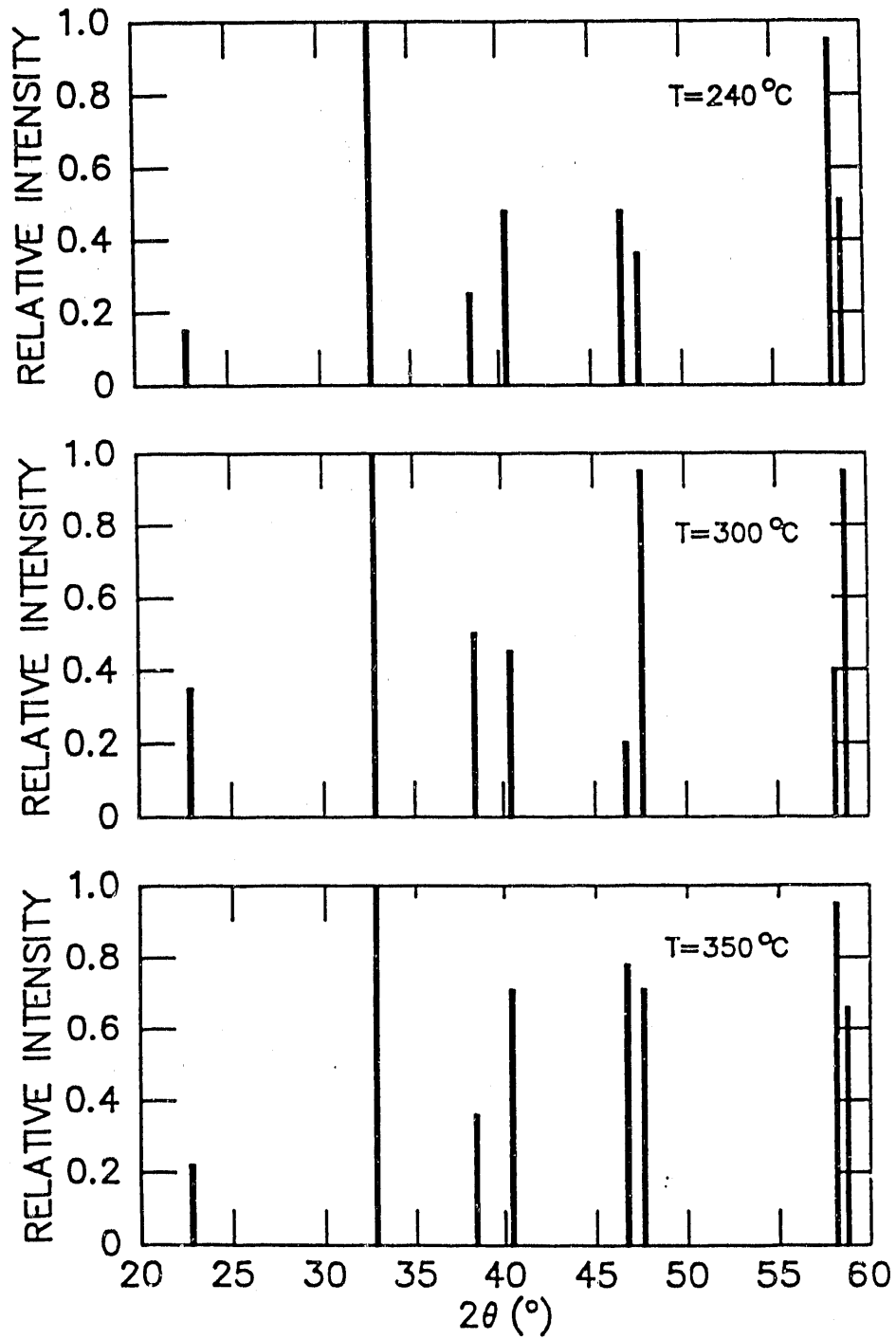
Figure 5





03873

Figure 5



03872

Figure 8.



END

DATE FILMED

03 / 05 / 91

